J. Hydrol. Hydromech., 71, 2023, 1, 49–63
https://doi.org/10.2478/johh-2022-0027

sciendo Journal of Hydrology and Hydromechanics Institute of Hydrology SAS

Reconstruction of the 1974 flash flood in Sóller (Mallorca) using a hydraulic 1D/2D model

Carys Thomas[1*], Ioanna Stamataki[2], Joan Rosselló-Geli[3]

[1] Department of Architecture and Civil Engineering, University of Bath, Bath, North East Somerset, BA2 7AY, United Kingdom.
[2] School of Engineering, University of Greenwich, Chatham Maritime, Kent ME4 4TB, United Kingdom.
[3] Estudis d'Arts i Humanitats, Universitat Oberta de Catalunya, 08018 Barcelona, Spain.
[*] Corresponding author. Tel.: +44 7794945764. E-mail: carys.a.thomas@bath.edu

Abstract: Flash flood events are common in the Mediterranean basin, because of a combination of rugged coastal topography and climatological characteristics. The Balearic Islands are a flood-prone region with the research area, Sóller (Mallorca) being no exception. Between 1900 and 2000, Sóller experienced 48 flash floods with 17 categorised as catastrophic. In Sóller, the local surface water network comprises ephemeral streams. These are natural water networks that only carry water during periods of intense rainfall. Using the available evidence from the 1974 flash flood, this research used Flood Modeller to simulate the event. The research developed a one-dimensional (1D) and a one-dimensional two-dimensional (1D-2D) model that assisted in the understanding of the behaviour of the ephemeral stream during the flood. Analysis of hydraulic parameters such as water flow, depth and velocity provided an appreciation of the interaction between the channel and floodplain. Model development aims to forecast the impending impacts of climate change and urbanisation.

The results suggest that the characteristics of Sóller's catchment area naturally encourage flash flooding and hence can be deemed a flashy catchment. The model demonstrates that the interaction between the channel and floodplain relies heavily on surface roughness of both areas. The model proves that if flood intensity increases with climate change, the extent of flooding and consequently the damage will become more severe.

Keywords: Flash floods; Hydraulic model; Documentary sources; Historical flood reconstruction; Hydrograph; Mallorca.

1 INTRODUCTION

Understanding the effects and severity of past flood events has been of interest to engineers, geographers, and the local communities for many centuries. Learning from past flood events is a step into making more informed decisions regarding flood risk in the present and future.

Flash floods are one of the most hazardous natural disasters (Sene, 2013). Due to the local climate of the Mediterranean, the frequency of flash floods is higher than the rest of Europe (Gaume et al., 2009; Gaume et al., 2016; Llasat et al., 2016). Between 1940 and 2015, Gaume et al (2016) collected information regarding 172 flash flood events that occurred only in the Mediterranean. Flash floods are usually caused by intense rainfall and are characterised by their localised nature and high speed. Over the years, people have described them as "walls of water". They are particularly common in mountainous areas occurring on previously dried river beds. The main challenge of these events is that due to their quick nature they are rarely captured or measured on-site and thus their effect can be even more devastating (Alcoverro et al., 1999; Costa, 1987; Creutin and Borga, 2003; Gaume and Borga, 2008).

The use of a hydraulic flood model allows for a numerical and visual representation of flood events. Having the freedom to explore various scenarios and mitigation solutions adds depth to the understanding of flash floods and their impacts. Using imported data or data manually collected from the field, factors such as topography, catchment areas, land use, and infrastructure can be modelled accurately for each site, allowing for the simulation of past and future flood events. The imminent impact of climate change is growing evermore severe, with extreme weather and a rise in sea level playing a critical role in flood risk. An increase in the frequency and intensity of rainfall inevitably increases the risk and severity of flooding (Mahmood et al., 2016). This coupled with the existing cyclonic weather induced by Mallorca's location and topography has the potential to be disastrous (Nunez, 2019).

Incorporating historical flood events when estimating the risk for future flood events can help with the associated uncertainty as it reduces the risk for the required interpolation of these values (Stamataki and Kjeldsen, 2021). Furthermore, looking into these events in more depth and modelling them numerically, can provide a baseline for flood paths, areas of greatest danger and the severity of potential effects. Building from these events provides realistic representations of possible future flood events. Recognising how flooding will impact communities is vital to ensure a safer future. The use of flood modelling therefore provides a helpful approach to understanding flood management and flood defence solutions (Wheater, 2002).

There has been a lot of research into reconstructing the peak flow of historical flood events. Researchers over the years (Elleder, 2010; Elleder et al., 2013; Herget and Meurs, 2010; Herget et al. 2014) have primarily focused on reconstructing the magnitude of historical flood events rather than creating an accurate representation of the river system hydraulics including the effect of hydraulic structures (e.g. bridges). Even though many of the aforementioned researchers have used the slope area method for the reconstruction of peak flows, the technique results in some simplifications. The complex hydrodynamic

effects of the river flow's interaction with its floodplains and hydraulic structures is not represented. Consequently, this can result in additional uncertainty associated with the reconstruction of the peak flow.

For the majority of cases, historical flood data and accompanying meteorological data is limited. The evidence primarily used in flood reconstruction includes epigraphic evidence (flood water levels marks), photographs and witness documentary sources (Elleder, 2010; Herget et al., 2014; Stamataki and Kjeldsen, 2021). These sources in conjunction with hydraulic models play an important role in reconstructing floods and predicting future impacts. Stamataki and Kjeldsen (2021) reconstructed 16 historical flood events in the city of Bath using a 1D hydraulic model. They used recorded peak flow values to calibrate the model and assessed the peak flow of historical flood events using epigraphic evidence in the city (flood marks). Thus they extended the annual maximum series of peak flow back to 1866.

Identifying risks and reducing vulnerability is key in reducing flood impacts. Vulnerability combines demographic, financial and exposure factors; hence it is clear that the flood severity is dependent on both flood and catchment parameters. Identifying these risks is often done by identifying and using peak discharge values to determine flood depths and extents. This can be completed using stage-discharge curves and/or one/two-dimensional hydraulic flood models (Moel et al., 2009). Results of both approaches can be translated into flood hazard maps which identify areas of concern.

This paper investigates the development of a hydraulic model to estimate the flood extent and effects of the 1974 flash flood in Soller (Mallorca) using available documentary sources. Hydrological and cross-sectional data were collected from different sources and the numerical model was calibrated using eye-witness records and photographic evidence. We discuss how a one dimensional (1D) hydraulic model enabled us to reconstruct numerically the 1974 historical flood and what we learnt from the model. Then the model expanded to a 1D-2D coupled model utilising DEM topographical data and was used to investigate the events flood extents. To summarise, the importance of using numerical models and the effort required to incorporate them in modern flood risk assessments is discussed and the uncertainty associated with this methodology is described. Additionally, the impact of climate change on the floodplain extents is assessed for future mitigations.

2 RESEARCH AREA

The research area is located on the western coast of Mallorca (Figure 1), adjacent to the Tramuntana mountain range, the highest of the island. With a surface of 50 km^2, the valley of Sóller is enclosed by mountains over 1,000 m a.s.l., a rugged relief close to the coast. This results in two different areas; the plain being the lowest and closest to the sea, and the mountain lying on the slopes of the mountain range.

Geologically, the plain is settled over quaternary alluvial soils while the mountains lie over Keuper and Muncheskalk materials, mostly calcareous and conglomerate rocks.

The rainfall in the area is determined by the Mediterranean geographical location of Mallorca. Annual amounts increase from the coast, averaging 600 mm/year, to the mountain tops, where averages reach 1,000 mm/year. There is a large interannual irregularity and an alternance of dry and rainy periods is very common. In terms of the rainfall seasonality, autumn is the primary rainy season, followed by spring and winter. Summer is the driest season of the year, with July having the lowest record of rainfall, usually 0 mm.

The geological and climatological conditions of the area have led to a water surface network of ephemeral catchments, known locally as “torrents” (Figure 2). Such streams are characterised by large infiltration rates (due to the karstified bedrock) and long dry periods. Runoff usually depends on the occurrence of heavy precipitation episodes (HPEs), which are common and result in flash flood events.

The valley’s main catchment is the torrent Major, resulting from the combination of three tributaries: torrent de Fornalutx, torrent de Biniaraix and torrent de’s Coll. The three tributaries meet in the middle of the town of Sóller and run towards the sea, discharging in the port of Sóller Bay (Figure 3). The torrent Major is 10.6 km long with a surface area of 49.3 km^2. Upstream the slope is steep whilst the final three kilometres run through the plain, which is almost flat. The average slope is 0.11.

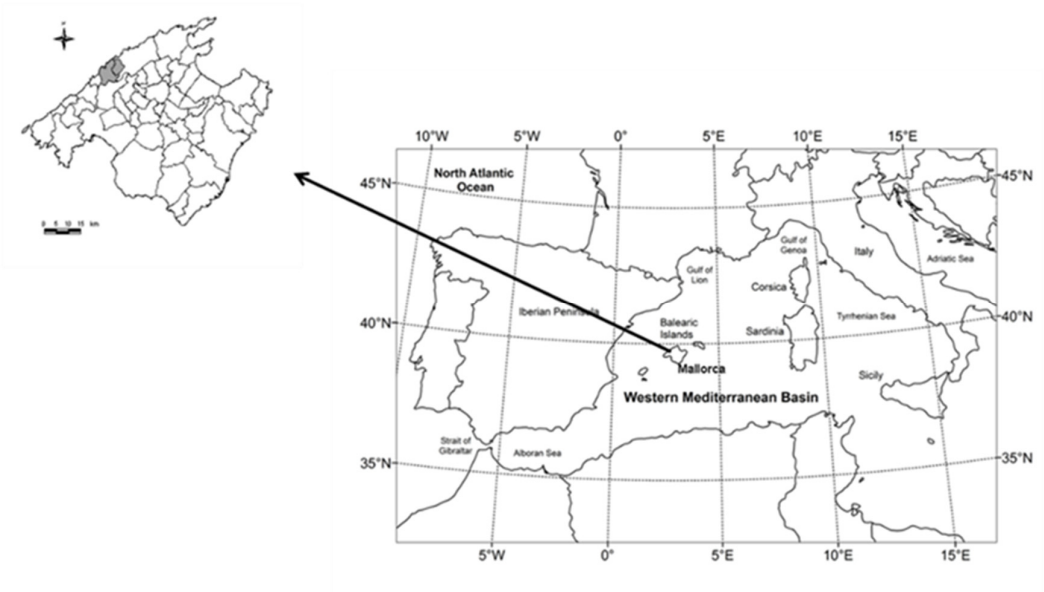

Fig. 1. Location of the research area in Mallorca and Mallorca within the Western Mediterranean (Rosselló-Geli and Cortés, 2021).

Fig. 2. Downstream section of Torrent Major and new Ca'n Repic bridge.

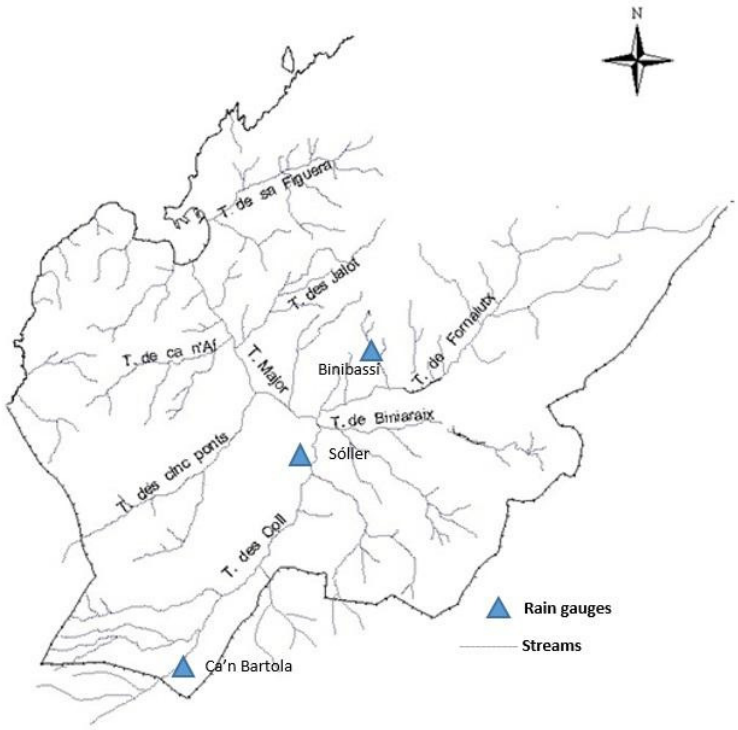

Fig. 3. Surface runoff system of the Sóller valley (modified from Rosselló-Geli, 2000).

The catchment has a low torrentiality coefficient (1.52), which indicates that it has a low ratio of the number of first-order stream to basin area (Romero-Díaz and López-Bermudez, 1987). Despite this, floods have affected the catchment since as early as the 17th century. According to a documentary source (Rullan, 1885), between 1640 and 1855, 13 floods affected the area, most often with catastrophic effects. Since 1900, 48 events have been identified (Rosselló-Geli and Cortés, 2021), with damages ranging from ordinary to catastrophic, following the classification by Barriendos and Llasat (2003); the latter being a flood that results in high infrastructure and economic costs and is of serious danger to the local population while the former is a flood that affects the closest area to the stream, causing minor damages in farming land and riverbed infrastructures.

3 STUDY EVENT

On March 30 1974, a significant area of the torrent Major catchment was severely flooded, primarily impacting the low-lands of the valley. The flood resulted from a sudden increase in surface water runoff which was related to heavy precipitation that commenced on March 29th across the island of Mallorca.

A low pressure region off the Algerian coast drove a flux of humid air towards the Balearic Islands, which upon collision with Mallorcian reliefs, resulted in intense precipitation (Figure 4).

Within the area of interest, precipitation commenced during the 29th with values of over 150 mm of rainfall recorded for the entire catchment. According to the Spanish National Meteorological Institute (INM), a maximum rainfall of 349.5 mm across 2 days was recorded in the area. Table 1 shows rainfall recordings for 3 different gauges within the area.

The high precipitation resulted in a sudden increase of the water levels within the catchment's ephemeral streams. The streams were overwhelmed causing flooding in the lowest area of the valley. Flooding of the "Torrent dels Cinc Ponts", located on the western side of the basin had a severe impact (Figure 3). Water levels breached the ephemeral stream walls and caused

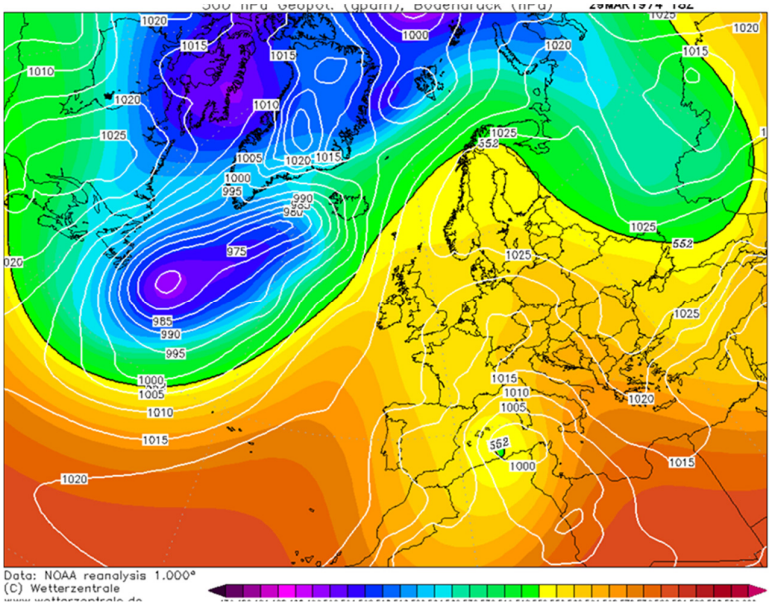

Fig. 4. Atmospheric situation March 29 1974 (Wetterzentrale, 2021).

Table 1. Rainfall distribution. Source: INM.

Code number and raingauge name	March 29th 1974	March 30th 1974	Total
B046 Binibassí	195 mm	154.5 mm	349.5 mm
B059 Ca'n Bartola	170 mm	46.5 mm	216.5 mm
B061 Sóller	165 mm	95 mm	260 mm


SÓLLER
SEMANARIO DE INFORMACIÓN LOCAL
INUNDACIONES EN LA HUERTA Y ES CAMP DE SA MAR
EL EXCMO. SR. D. ENRIQUE RAMOS, GOBERNADOR DE LA PROVINCIA, VISITO LA ZONA AFECTADA
Información en pags. centrales

Fig. 5. Screenshot of the cover of the Semanario Sóller showing the effects of the flood (BMS, 2021a).

flooding of the right hand side (looking downstream) of the "torrent Major". This had a considerable impact on the main road to the port of Sóller and the houses and orchards in proximity to the flooded area (Figure 5).

Sóller citizens accused neglected and inconsiderate infrastructure for causing the flood. These included a lack of maintenance of irrigation canals and ditches on the agricultural land and the inconsiderate construction of the main road leading from Sóller to the harbour which destroyed the historical water drainage system that encouraged rainwater to move into the ephemeral streams. From a meteorological perspective, the cause of the flash flood was the prolonged precipitation the week prior to the flood which resulted in complete saturation of the ground during the flood event.

The associated societal impacts were most severe and expressed, with reports reaching national newspapers. Domestic dwellings and agricultural land were flooded, two women had to be rescued from their home which was unreachable due to high water levels, and the connection between Sóller and its harbour was temporarily hindered due to both road and tram line damages, in addition to water and debris blockages. The flood damages were valued at approximately 45,000,0000 pesetas, equivalent to €4,000,000 today. These were primarily related to the valley's agricultural industry and the coastal tourism industry.

4 METHOD

To estimate flood extents both a one-dimensional (1D) and a one-dimensional two-dimensional (1D-2D) linked model were developed. A hydraulic model is a numerical representation of the movement of a fluid through a system and it allows the

understanding of the corresponding hydraulic behaviour (Stamataki and Kjeldsen, 2020). It numerically simulates the flow of water through a river and how the water interacts with the channel, the floodplain and surrounding infrastructure.

The 1D model was initially developed, followed by the construction of the 1D-2D linked model. Once both models were constructed and calibrated, the model was used to further understand the behaviour of ephemeral streams under different conditions and investigate the impact of climate change.

4.1 Model

The research used Flood Modeller; a computational programme that allows for the numerical representation of water flow through channels, across floodplains and via drainage systems, thus permitting for surface flow analysis in 1D and and 2D. The construction of a 1D-2D linked model is also possible, where the river channel is represented in 1D, whilst the floodplain and surrounding catchment is represented in 2D via the incorporation of a digital elevation model (DEM). This is a topographical model. The dynamic link between 1D and 2D models means that if water overspills the 1D channel, it becomes an input in the 2D model. 1D values that overspill to the 2D floodplain are numerically factored to ensure they are representative of the 2D domain (Jacobs, 2020). Flood Modeller was chosen as the primary research software as it allows the development of a realistic model despite limited input information.

The governing equations in Flood Modeller are the 1D Shallow Water equations, also known as the Saint-Venant equations (Eq. 1 and Eq. 2) (Jacobs, 2020). These are derived from depth-integrating the Navier-Stokes equations assuming that the length scale of our system is much greater than the vertical length and express the conservation of mass and momentum of a water body. The Manning's equation is also used in solving the normal depth boundary condition in addition to describing the interaction of flow with infrastructure.

$$Mass\ Conservation \rightarrow \frac{dQ}{dx} + \frac{dA}{dt} = 0 \quad (1)$$

$$Momentum\ Conservation \rightarrow \frac{dQ}{dt} + \frac{d}{dx}\left(\frac{Q^2}{A}\right) + gA(So - Sf) = 0 \quad (2)$$

where Q is the flow rate (m^3/s); x is the longitudinal channel distance (m); A is the cross sectional area (m^2); t is the time (s); g is acceleration due to gravity (m/s^2); So is the bed slope (m/m) and Sf is the friction slope (m/m).

4.2 Model construction

Building a historical hydraulic model is not an easy task and some fundamental input data are required in order to begin modelling. The data required for the 1D and the coupled 1D-2D models are described below.

4.2.1 1D model construction

For the base of the 1D model, the data was provided by the Climatology, Hydrology, Natural Hazards and Landscape Research Group at the University of Balearic Islands (UIB) and included:

- Data related to rainfall and peak flow of the 1974 flood and an image of the hydrograph from a flood event in Sóller in 1978 (Rosselló-Geli, 2000).
- Cross section geometry of the ephemeral stream along its length, with corresponding stream roughness values.
- Digital elevation model (DEM) data of local topography to a 2.5 m resolution (IDEIB, 2021).
- Location, dimensions, and cross sections of the bridge at the lower boundary of the model (AMS, 2021).

Figure 6 shows the simplified setup used when using a hydraulic model to represent a river. This includes defining an inflow hydrograph, river cross sections, bridges and a downstream boundary condition. These are all defined relative to the river's length. Each step is explained analytically below.

Inflow hydrograph: The first schematic (Figure 6) represents the inflow hydrograph. Flood hydrographs are graphs showing how a catchment responds to a rainfall event by plotting the flow rate over time for the duration of the flood. In hydraulic models it represents the model's upstream boundary condition - in this case at Barona Bridge - and it determines the propagation of the water flow along the system. The model's results are highly dependent on flood hydrographs as the intensity of the inflow dictates the characteristics of the flood. During the 1974 flash flood, no flood data were recorded as there were no flood gauges at the time. However, by the time of the 1978 flood event, the gauges were in operation, and the 1978 flood event was accurately recorded. Due to lack of data, the assumption was made that the shape of the hydrograph from 1978 was representative of that for the 1974 event. This relates to similarities in catchment's response time to different rainfall and flood events. Therefore, the rate of rise and fall of the flow corresponds to the 1978 flood events. The recorded peak discharge of the 1978 flood via gauges was 30.86 m^3/s and thus the calculated and scaled peak discharge of the 1974 flood was 114.22 m^3/s. A ratio between the two values was defined, and the 1978 hydrograph was scaled to represent the peak discharge of the 1974 flood (Figure 7). The rising limb of the hydrograph begins at 17 hours, the time taken between the initial precipitation on the catchment and the beginning of the initiating discharge.

River cross sections: The second and fourth schematics (Figure 6) refer to the stream's cross sections. These are required at different locations along the stream to define the river channel, as shown on Figure 8. The channel geometry and surface roughness (Manning's coefficient) are input parameters required in order to model the river. Longitudinal distances between each section are also defined. The model presented in this work, consisted of 8 cross-sections, labelled Cross section 1 (CS1) – Cross section 8 (CS8) where CS1 is furthest upstream whilst CS8 lies at the downstream boundary. Figure 8 is

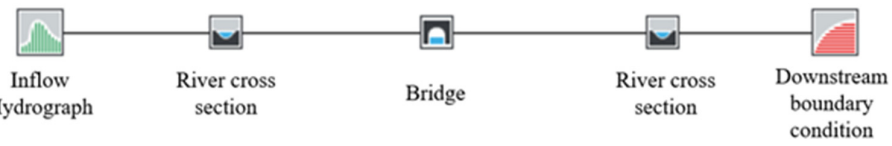

Fig. 6. Schematic showing a simplified setup with an inflow hydrograph, a river cross section, followed by a bridge, another river cross section and finally a downstream boundary condition.

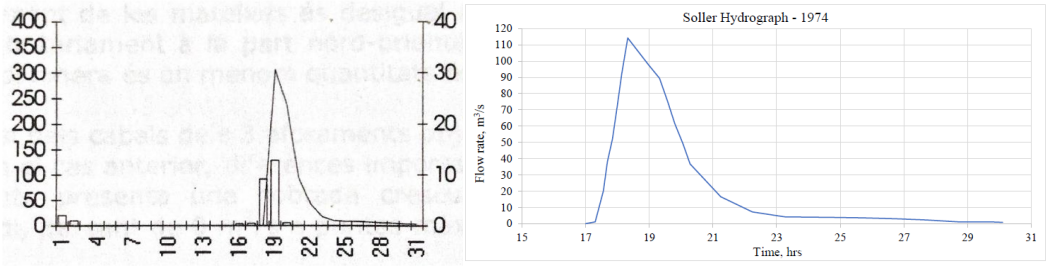

Fig. 7. Scanned hydrograph of the 1978 flood (left) from Rosselló-Geli (2000) and scaled hydrograph of the 1974 flash flood event (right).

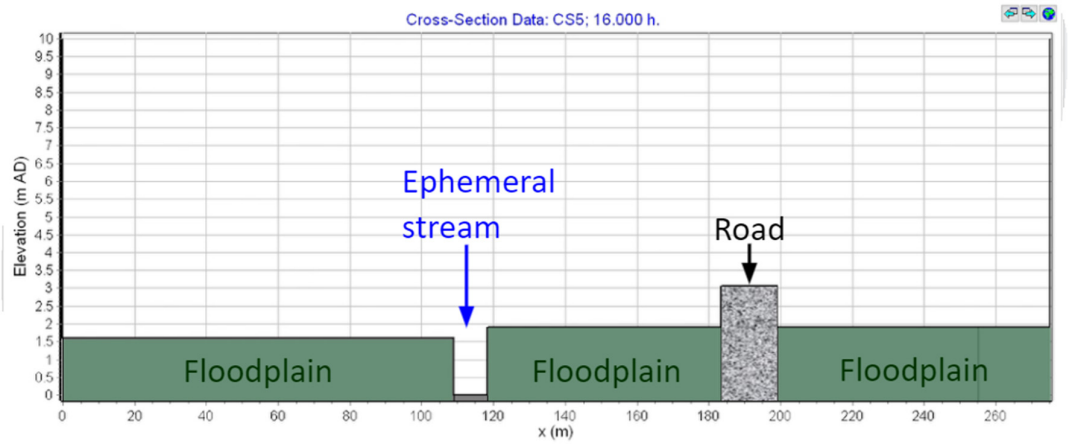

Fig. 8. Example of a river cross section definition in Flood modeller showing the different materials (floodplain, road) and the location of the ephemeral stream.

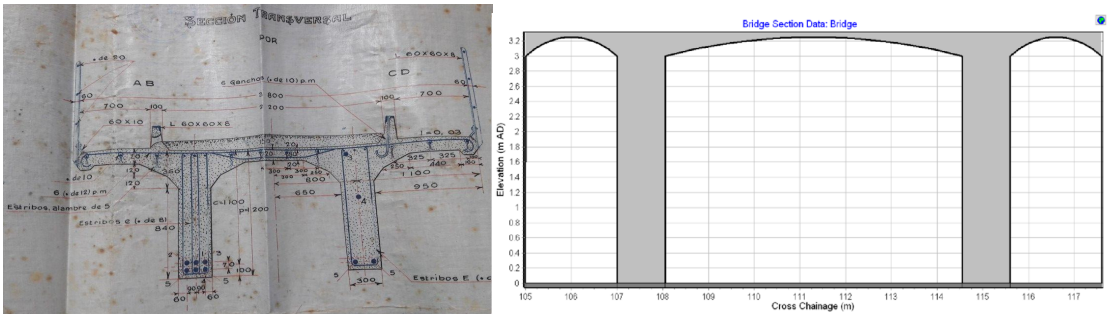

Fig. 9. Blueprint of Ca'n Repic bridge's dimensions (AMS, 2021) (left) and example of the numerical representation of Ca'n Repic bridge in Flood Modeller (right).

an example of CS5 where it shows the defined river cross section of the ephemeral stream, the elevated road and floodplains.

Bridge: The third schematic relates to the definition of hydraulic structures and in this case bridges within the modelled section of the river/stream. To define a bridge in Flood Modeller, firstly the bridge's dimensions need to be determined and the location of the bridge relative to the adjacent cross sections specified. Incorporating the bridge within the model was a vital step of the research as bridges often cause obstructions during flood events and have an impact on the flow of water. Cross sections CS6 – CS8 in the model therefore primarily relate to the Ca'n Repic bridge (Figure 9).

Downstream boundary condition: The last schematic in Figure 6 is the downstream boundary condition which provides the conditions at the end of the model. Here the slope of the stream's bed is defined and the flow is characterised in terms of depth and velocity. This primarily relates to the numerical calculations of the hydraulic model.

A plan view of the finished model and the location of the 8 different cross sections can be seen in Figure 10.

4.2.2 1D-2D linked model construction

Constructing the 1D-2D linked model follows the same schematic as described above for the 1D model, however the geometry of the river cross sections differs. The 1D-2D cross sections now only represent the river channel itself and hence are modelled as a simple rectangular shaped channel. The floodplain is incorporated via the provided 2D 2.5 m resolution DEM data (IDEIB, 2021), which clearly defines the river's course and the surrounding floodplain. The two-dimensionality of the DEM provides an accurate representation of the flood path which is dictated by the topographical characteristics.

Initially, the DEM data is imported and the river is outlined by a shape file. The cross section geometries, bridge location and boundary conditions are also incorporated within the 1D

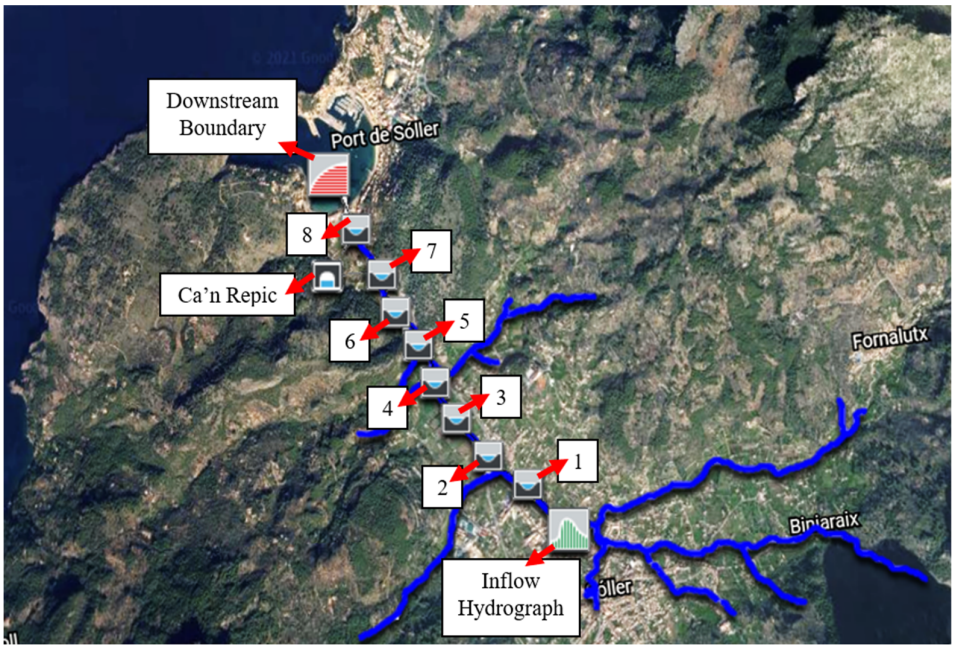

Fig. 10. Plan view of the stream showing the location of the different cross sections (CS1–CS8) (Google Earth, 2021).

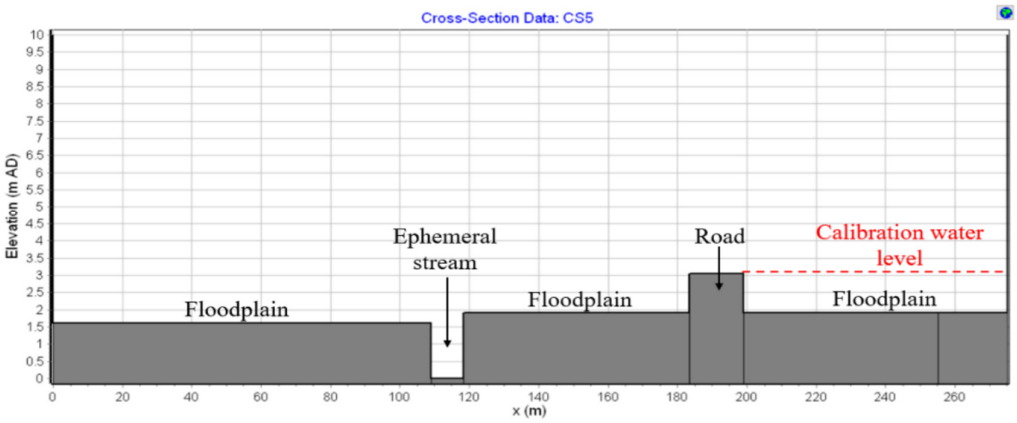

Fig. 11. Cross section 5 (CS5) with calibration point.

model. To concentrate the DEM data to the area of interest, an active flood area is assigned around the river channel. The connected 1D river data and 2D DEM are then linked within the model.

4.3 Model calibration

Once all information is inputted into the modelling system, the process of model calibration can begin. This is the process of adjusting the unknown factors in the model until the model can provide a good description of the river system. The purpose of calibrating a flood model is to ensure it is an accurate and valid representation of the stream and the system hydraulics during the flood event. For the 1974 flood event, a calibration point on agricultural land at cross section 5 (CS5) was selected. An eyewitness (the land owner) stated that the flood level reached 1.5 m within his field, a value that was also supported by photograph measurements from the flood (Figure 11).

With a fixed inflow hydrograph and stream geometry the changeable parameters were the stream's roughness. The river roughness was therefore adjusted within some acceptable uncertainty markets in order for the simulated model water levels to match (within 5%) the known calibration point (1.5 m water depth in the floodplain of CS5). An important factor for calibration was the saturation level of the ground prior to the flood. Due to the significant rainfall measurements recorded the week prior to the flood event, it was assumed that the floodplain was partially if not fully saturated. The floodplain saturation provides additional water volume to the catchment and therefore, to incorporate this into the model, a constant water depth of 0.1 m was assumed to reside on the floodplain.

To calibrate the 1D-2D model, the 1D calibrated simulation results are incorporated as an input file into the 2D simulation. The 2D analysis uses the resulting 1D hydraulic parameters to produce the 1D-2D linked results.

4.3.1 Testing

The calibrated model allowed for analysis of the flood extent of the 1974 event in addition to further research into the behaviour of ephemeral streams and the impact of climate change.

The testing schedule was as follows:

1D simulation of the 1974 flood event (the calibrated model)
1D-2D linked simulation of the 1974 flood event
1D-2D simulation of the impacts of climate change

With climate change growing ever more severe global temperatures and frequencies and magnitudes of extreme weather events are increasing, especially high precipitation events across the Mediterranean (Cos et al., 2022; Tuel and Eltahir, 2020). The rise in temperature increases the moisture content of the atmospheric air (Mahmood et al., 2016). For each degree of temperature rise, the air's water vapour capacity increases by approximately 7%. (Clark, 2011). Although it is recognised that the atmosphere's moisture content does not increase homogeneously, nor does an increase in water vapour capacity result directly in larger volumes of rain, in order to conduct a simplified exercise representing climate change, the input flow was increased by 7%.

5 RESULTS

The aim of this research project was to reconstruct the historical flood of 1974 in order to obtain a more accurate assessment of the effect of the flood, which would prove useful in understanding the contemporary flood risk of Sóller.

5.1 1D Model results

It is important to note that the 1D model reconstructed the river system as it was at the time of the flood using a variety of sources.

Figure 12 shows the flow rate (blue), velocity (green) and water depth (red) at cross section 5 (CS5 - calibration point). It is interesting to indulge into the details of what is happening at this specific cross section. From a fundamental perspective, conservation of mass states that matter cannot be created nor destroyed though it may be transformed from one form to another (e.g. by a chemical or nuclear process). Thus in response to the increasing flow (first hour of flash flood event), one of two things needs to happen to satisfy continuity, the conservation of matter: (i) either the velocity needs to increase if the cross sectional area remains unchanged and/or (ii) the cross-sectional area must increase in order to for the velocity to decrease but the flow to remain constant throughout the system. Looking at the graph in more detail, the water remains in the ephemeral stream channel until 18.5 hours, restricting the cross-sectional area, resulting in an initial steep rate of velocity increase. The increase in the velocity of the flood water is therefore the stream's initial response. The velocity reduces severely once the water breaches the stream's banks and extends to the floodplain and hence we see it accompanied by an increase in the water depth. After the flow rate reaches its peak flow, the maximum value, the water remains on the floodplain, with the water depth (red line) decreasing at a slow rate of approximately 0.14 m per hour. The velocity also continues to decrease. This represents the hydrograph's decreasing flow rate and the friction asserted on the flow from the floodplain and slope. The secondary peak in velocity apparent at 30.5 hours occurs due to the sudden restriction in the cross sectional area where the water begins to flow only through the stream channel once again.

The event's rapid onset and steep slope of the hydrograph's rising limb highlights the severity of the flash flood event. Figure 13 is a series of screenshots from the simulation of the event at CS5, the calibration point. The 14 screenshots are at approximately 1 hour intervals, from 17 to 31 hours, in which 17 hours is the beginning of the flood readings. Images 1–4 highlight the shear increase in flow and water depth, whilst images 5–14 demonstrate the slower rate of falling water depth. It is important to note the velocity increase discussed from 17 to 18.5 hours where the water remains in the stream channel (Screenshots 1 and 2) and the flow is restricted within the stream's cross sectional area. Looking at Screenshot 3, the water has breached the stream's banks and has now extended to the floodplain. This relates to the sudden drop in the velocity discussed earlier and the corresponding increase in the water depth. The described decreasing flow rate of the hydrograph accompanied by the slow decrease of water depth and velocity is apparent in Screenshots 4–13. Finally, the secondary peak in velocity at 30.5 hours is apparent in Screenshot 14 when all water returns back to the stream channel.

While running the model, another noteworthy factor was that the upstream floodplains of the model were submerged for a greatest length of time with a depth of 3.4 m. Moving downstream through the cross-sections, the submersion time and water depth reduced, with only a maximum depth of 1.96 m across CS6, CS7 and CS8.

The maximum velocity in the channel and on the floodplain occurs at CS8 with values of 1.21 m/s and 1.14 m/s respectively. The floodplain velocity is only sustained for a short period of time; however, its impact remains significant. The average velocity across the floodplain at all cross-sections during the average 4 hours submersion time is 1.06 m/s, which is 0.19 m/s above the average velocity throughout the entire flood event duration.

Finally, in order to assess the interaction between the bridge and ephemeral stream's flow, a comparison was made between CS6, situated directly upstream of the bridge and CS8, situated directly downstream of the bridge in terms of water depth (Figure 14 left) and velocity (Figure 14 right). By comparing the values at the two different locations (CS6 is upstream and shown in blue and CS8 is downstream and shown in red), it is evident that the bridge structure has a significant impact on the flood event.

A way to understand the effect a bridge has in a water stream is to calculate its afflux which is the rise in water level on the upstream side of the bridge (CS6) caused by the effective reduction of the channel's width. Looking at the left image, there is a 0.41 m surge in water level upstream of the bridge location. This suggests that the bridge is restricting the movement of water and causing the water depth to accumulate and increase on the upstream side and thus it can be identified as a significant obstacle in the flow during a flash flood event. This occurs between times of 19.5 and 23.2 hours, which correlates with the times that the water is on the floodplain, illustrated in Figure 13. While this blockage is obvious on the left figure by an increase in water depth, it also translates to a decrease in velocity of 0.61 m/s between CS6 to CS8 during that time. This sudden decrease in velocity can once more be explained using the continuity equation where, as the water depth increases, the cross sectional area is increasing and thus the velocity must decrease to satisfy continuity.

5.2 1D-2D linked model results

The results for the 1D-2D 1974 flood event and the climate change event models are described below. Figure 15 provides a reference for the results presented highlighting important cross section locations (CS1–CS8) and the location of the Ca'n Repic bridge.

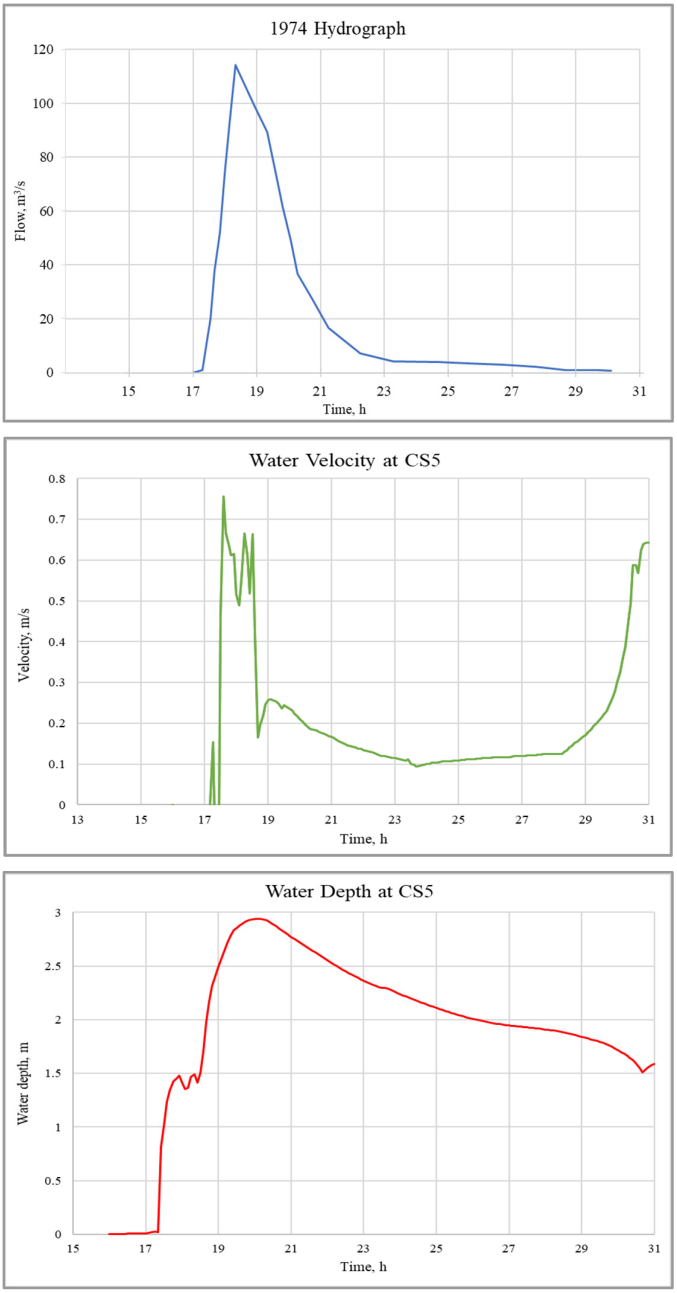

Fig. 12. Simulated flow rate (blue), velocity (green) and water depth (red) at cross section 5 (CS5 - calibration point) during the 1974 flash flood event.

5.2.1 The 1974 flood event

Following the successful modelling of the 1974 flash flood, the 1D (one-dimensional) model was coupled with a 2D (two-dimensional) model to simulate the hydrodynamic behaviour of the flood along the floodplains more accurately. Figure 16 shows a series of screenshots simulating the flood extents of the event on the floodplains. The 8 screenshots are at intervals of approximately 2 hours, from 17 to 31 hours and the different colours (see legend) represent different water depths along the floodplain ranging from 0.01–0.111 m with dark blue to 1.929–2.028 m in red.

The results produced by the 1D-2D model are consistent with the local topography and results from the 1D simulation of the flood. Figure 16 clearly shows the influence of the surrounding topography on the flood path. Low lying areas correspond to vast flood extents, whilst the section running between the two mountain ranges experiences less flooding as it is clearly constricted by the steep adjacent land. The worst flooding occurs between CS3 and CS5, with a maximum water depth of 2.5 m whilst in general the right hand side of the river banks experiences greater depths than the left hand side, due to the local topography. Further to this, looking more specifically at the bridge, the modelled water depths upstream of the bridge were greater than those downstream which implies that the bridge's blocking effect extends significantly upstream. The velocities were greater downstream of the bridge which successfully correlates with the restriction of depth caused by the

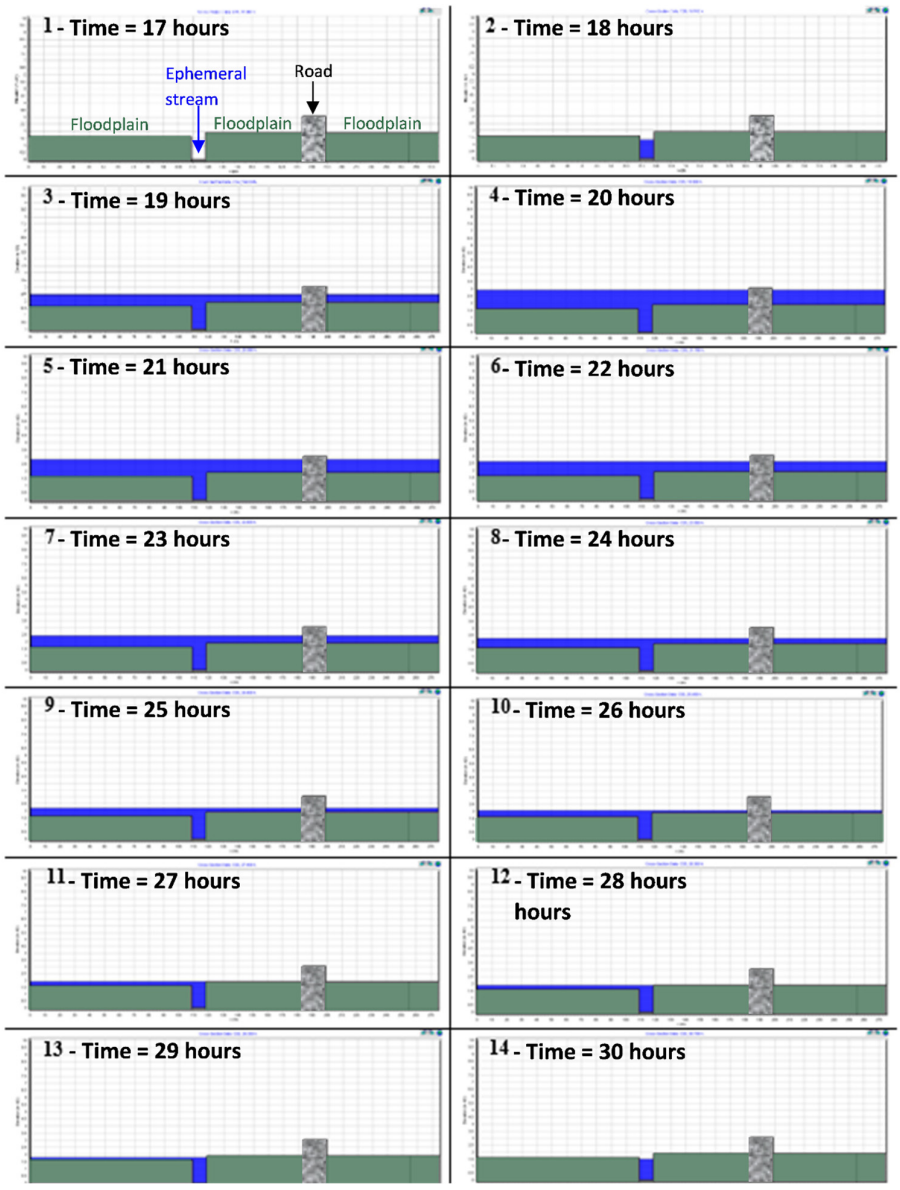

Fig. 13. 1D model simulation results at CS5 from 17 hours (beginning of flash flood event) to 30 hours.

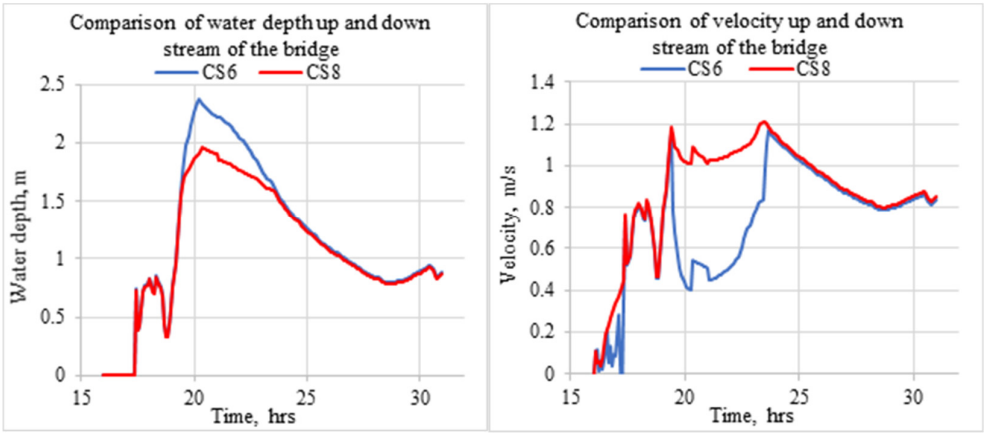

Fig. 14. Simulated water depth (left) and velocity (right) at cross sections CS6 (upstream of the bridge - shown in blue) and CS8 (downstream of the bridge -shown in red) during the 1974 flash flood event.

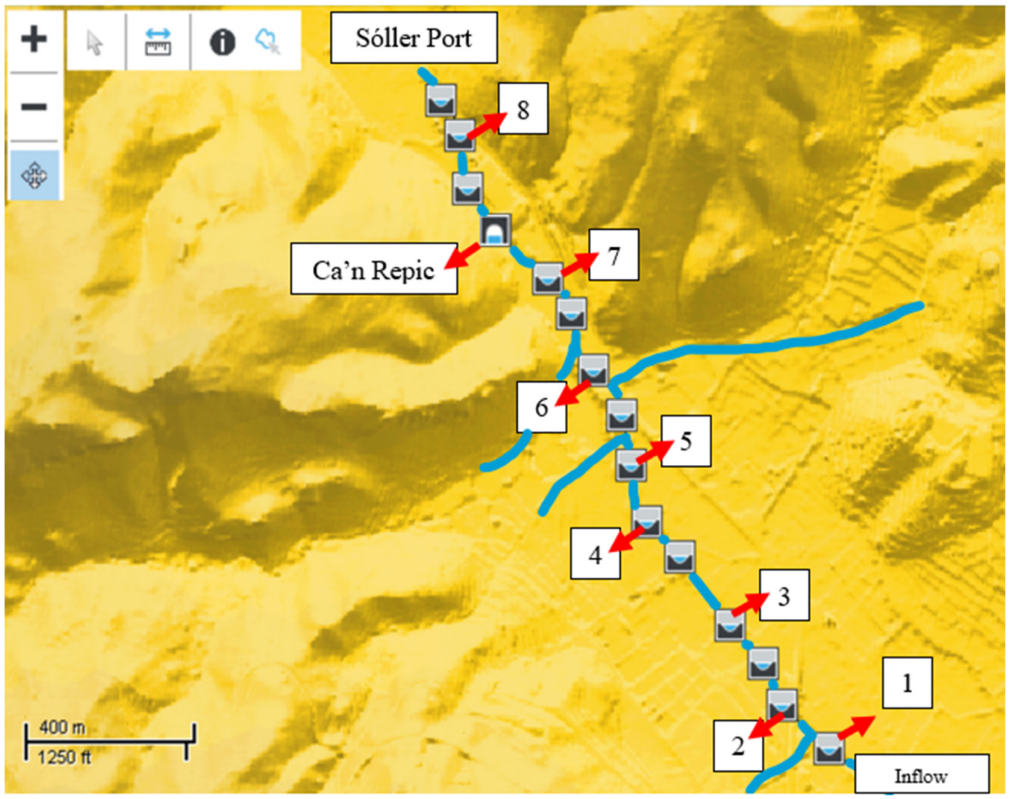

Fig. 15. Reference map for the 1D-2D linked model results.

bridge and satisfies continuity. Finally, it is interesting to compare figures 13 and 16 especially the initial hours of the event. They demonstrate the shear speed of the flood occurrence with both highlighting that the floodplain is inundated by 19 hours, only 1.5 hours after the start of the flood event.

5.2.2 Impact of climate change

As previously mentioned, increased precipitation and more extreme weather conditions accompany climate change. The hypothesis tested is that with Mallorca already experiencing cyclonic weather, and this being a prominent cause of flooding, the impact of climate change could be disastrous (Nunez, 2019). Recognising the magnitude of the expected increase will assist future predictions and consequently aid with future flood mitigation efforts.

Comparison of the 1D-2D model results for the 1974 flood and climate change tests illustrate the difference in flood extent (Figure 16). Figure 16 shows the flood extent data from 1974 in blue and compares them with the expected flood extents due to the 7% flow increase, shown in green. Figure 17 shows 8 screenshots at approximately 2 hours intervals, from 17 to 31 hours and the different colours (see legend) represent different water depths along the floodplain ranging from 0.01–0.23 m with light blue to 1.97–2.19 m in blue and 0.01–0.27 m in light green and 2.36–2.62 m in dark green.

This figure shows that climate change will only exaggerate the effects of the 1974 flood, thereby posing future risks to Sóller. Climate change combined with an expected increase in urbanisation will definitely result in an overall increase in floodplain velocities and water depths, which enhance the dynamic pressure and the impacts on the floodplain as well as the impact on the existing infrastructure. These are scenarios identified as being detrimental to Sóller due to its increased risk to the community's livelihood, its present and future economy and the infrastructure.

6 DISCUSSION

The hydraulic model has shown the significant impact the 1974 flood event had on Sóller. The flood extent, velocities and depth are all directly influenced by the flood hydrograph and the surrounding catchment. The initially steep catchment promotes rapid movement of water whilst the downstream low-lying and textured catchment reduces velocities and encourages pooling. The shape of the inflow hydrograph demonstrates the falshiness of the event; the peak discharge is reached only a mere hour into the beginning of the flooding records. This natural encouragement of flash flooding deems Soller's catchment as flashy, that is, *"a catchment area that, because of geographic, topographic, and geological factors, shows an almost immediate response to intense rainfall, resulting in a flash flood*" (Werner and Cranston, 2009). It can be concluded that the town's flood risk is permanent.

CS1–CS4 are most heavily populated in terms of infrastructure and population, with the density wilting from CS5 onwards. The proximity of residence to the stream deems this vicinity as high risk. Water levels reach the ground floor of homes and local businesses, consequently having devastating financial and wellbeing impacts. In addition, it is not compulsory to have flood insurance for a property within flood zones in Sóller hence flood damages place an enormous financial burden on property owners. With regards to the wider outlook, it is not compulsory for any property owner to disclose to potential

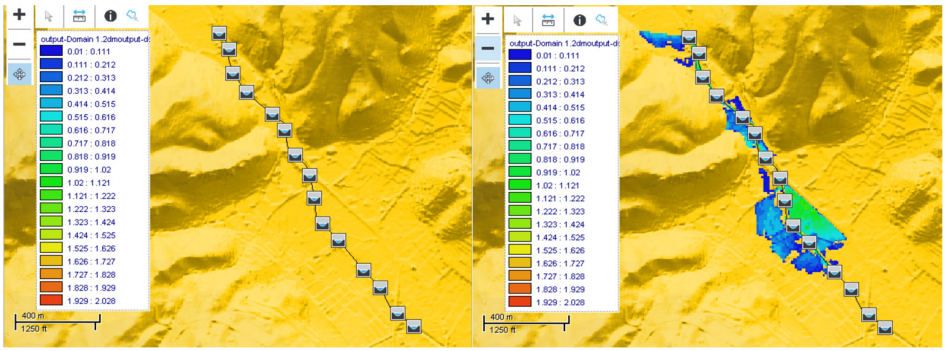

Time = 17 hours Time = 19 hours

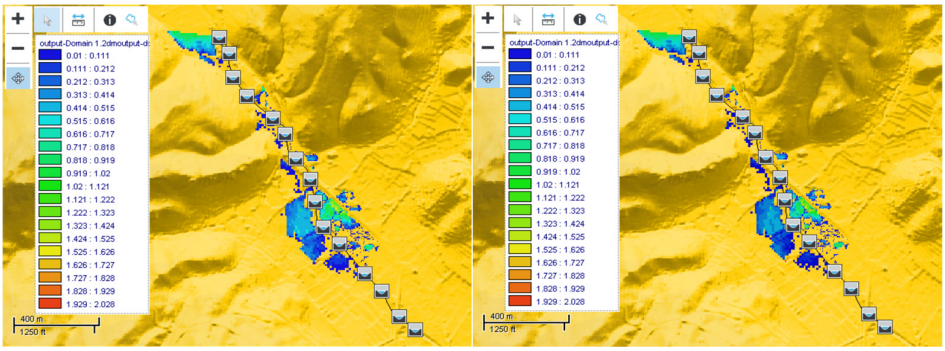

Time = 21 hours Time = 23 hours

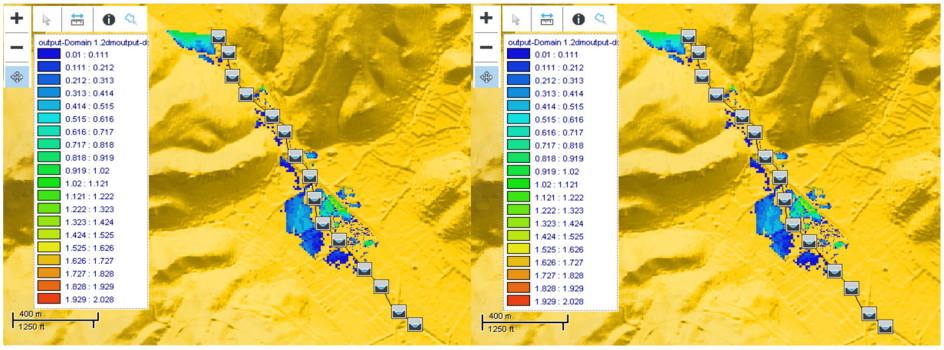

Time = 25 hours Time = 27 hours

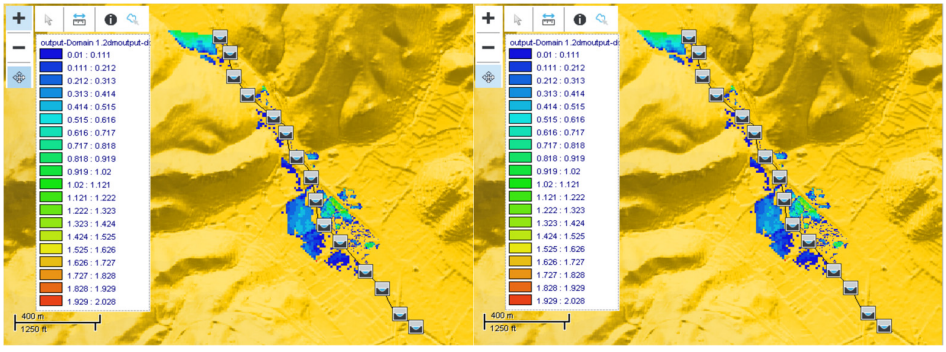

Time = 29 hours Time = 31 hours

Fig. 16. 1D-2D model simulation showing the flood extent during the 1974 flood. The different colours in the model represent water depths along the floodplains ranging from 0.01–0.111 m with dark blue to 1.929–2.028 m in red.

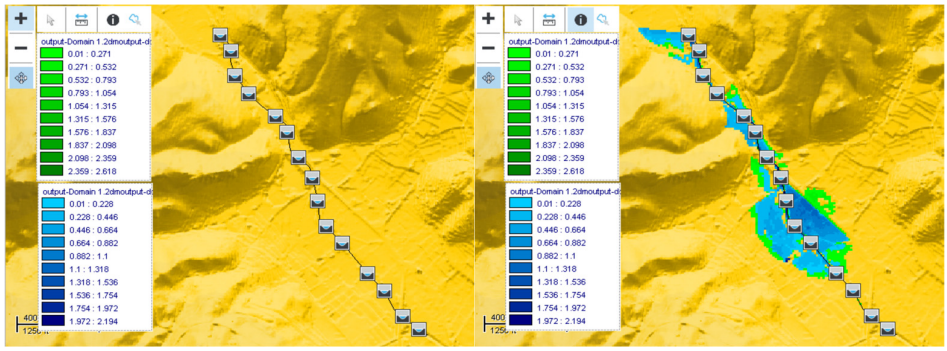

Time = 17 hours Time = 19 hours

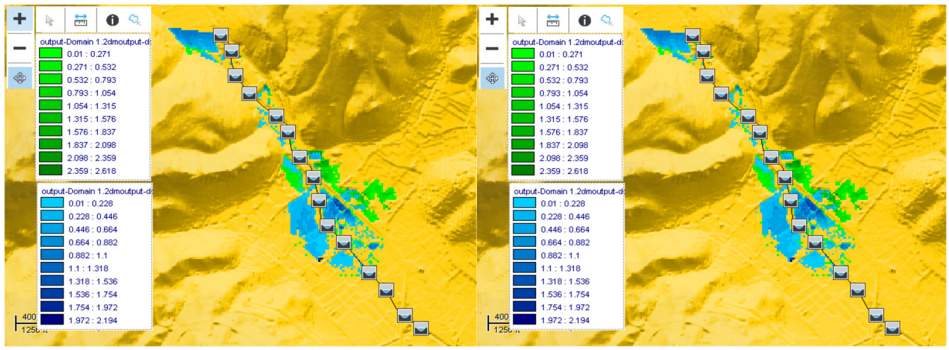

Time = 21 hours Time = 23 hours

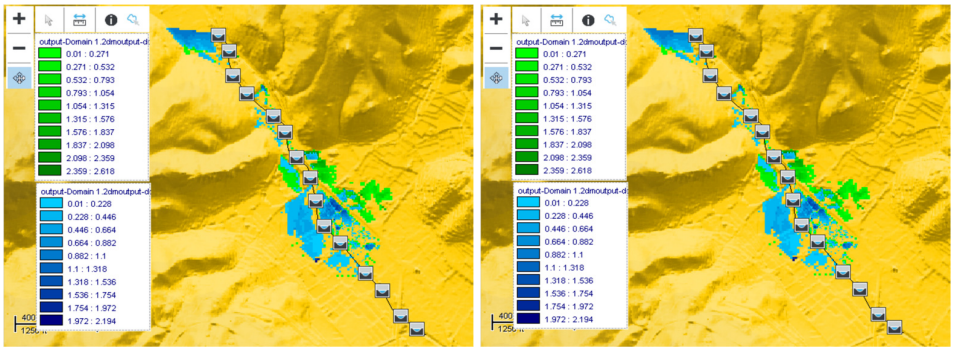

Time = 25 hours Time = 27 hours

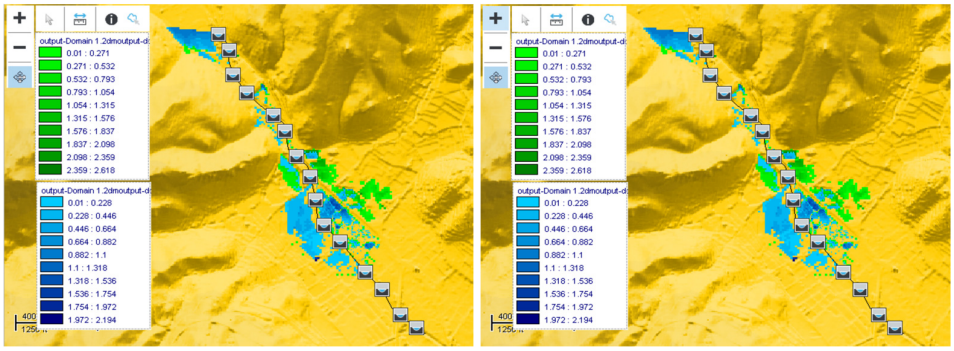

Time = 29 hours Time = 31 hours

Fig. 17. 1D-2D model simulation comparing the 1974 (blue) flood to the effect of climate change (green). The different colours represent different water depths along the floodplain ranging from 0.01–0.23 m with light blue to 1.98–2.19 m in blue and 0.01–0.27 m in light green and 2.36–2.62 m in dark green.

buyers that the property resides in a high-risk flood location which subsequently reduces community flood awareness and increases vulnerability (Rosselló-Geli, 2021).

The resulting significant period of submersion may result in ground saturation and an increase in the level of the groundwater table. Saturation disturbs and degrades the soil's nutrient levels which can consequently damage agricultural crops and biodiversity. Extensive submersion of crops will not only eliminate valuable community food resources, but impact the financial yield available on such products. An increase in the groundwater table will result in an increased risk of imminent future flooding due to current ground saturation. Pressure exerted onto low-lying infrastructural components could result in significant damage. To exacerbate the impacts, the flow magnitude and velocities witnessed will result in soil erosion which will reduce soil stability and hence increase Sóller's exposure to flooding.

The velocity reaches its peak within the channel for all cross-sections, with a maximum peak at CS8. A higher velocity transports more debris and sediment, attributing to blockages and increasing flood risk. The ephemeral stream contains no flow under normal conditions, therefore despite the low magnitude of the velocity, the sudden increase may exert unique pressures on the channel. The peak velocity on the floodplain also occurs at CS8. The velocity is only sustained for a short period, but it remains to have the capacity to cause damage due to the dynamic pressure of the water flow.

The hydrostatic pressure exerted by the water depth and flood submersion time will impact both the channel and the floodplain infrastructure. The maximum pressure occurs at CS1, at a value of 8.63 kilopascals (kPa). This represents only 21% of the minimum pressure required to crush limestone (Pabon, 2019). Despite the pressure weakness, pressure accumulation due to submersion time has the ability to disrupt the structural integrity of the channel and surrounding infrastructure. This coupled with bed and wall erosion and infrastructure scour will only worsen the effects.

Further to this, the main road to the coast is flooded for approximately 3 hours, thus temporarily causing traffic disruption and dangerous driving conditions. Additionally, it was reported locally that the flood structurally damaged the road thus, causing further disruptions and economic impacts (BMS, 2021b). The local tram line that also runs alongside the road was also flooded for over 3 hours.

Considering the time of the flood event, it is unlikely that any sufficient or sophisticated rescue and medical resources were available. Socially, this would have caused stress and worry within the community. These social impacts in conjunction with the previously mentioned economic effects would have had a great impact on the communities wellbeing and livelihoods. Further to this, the 3 consecutive catastrophic floods of 1972–1974 would have likely reduced the town and community resilience, hence the 1974 flood could have been more devastating than expected.

6.2 Model limitations

The primary limitation of the hydraulic model relates to the limited information available regarding the 1974 flash flood in Sóller. The available documentary sources of (eye-witness flood mark, approximate flood reach locations) increase the uncertainty associated with the results. Additionally, mirroring the 1978 flood hydrograph introduces some further uncertainties and more in depth research is required into the shape of the hydrograph for the area. To reduce uncertainties, comparing a model with accurately collected data to the same scenario but with less reliability will highlight anomalies and suggest improvements.

Furthermore, a limitation of the 1D Model relates to the one-dimensionality assigned to the floodplain. Its nature prompts the assumption that the inflow hydrograph is input across the entire cross-section, whereas in reality the water would only enter at the streams channel. Modelling in 1D also assumes a constant water level rise despite infrastructure blockages and due to the input, set flood reach boundaries. This restricts the simulation of a natural flood reach and path and therefore does not allow for an organic flood progression and representation. These limitations however, are overcome in the 1D-2D linked model. A progression of the research could examine the influence of the 1D limitations by comparing the 1D and 1D-2D model results.

Generally, research does not consider inevitable river blockages such as trees and debris, which will provide obstruction. Blockages are unpredictable and vary depending on the catchment and flood severity however they would likely intensify flood's impact. The model assumes that debris does not provide any further obstruction. However, this is not a realistic view and must be considered as an intensifying factor.

7 CONCLUSION

This research highlights the significant effects of flash flooding on Soller, Mallorca. It clearly demonstrates that both catchment and topographical characteristics play a significant role in flood parameters and thus impacts. The degree of interaction between the flood path and surrounding infrastructure determines the scope of impacts and the risk of damage. Due to the densely populated upstream catchment, this increases vulnerabilities.

The research shows the importance of hydraulic modelling in informing future flood risk within the area. Climate change will lead to an increase in the frequency and magnitude of extreme weather and thus will lead to more flash flood events. With regards to Soller, this will widen and deepen flood paths, hence potentially worsening flood effects. Flash flooding will continue to be of significant concern in Soller and therefore it is vital to increase awareness and encourage action to be taken.

Flooding is a multi-disciplinary hazard that interests geographers, engineers, social scientists and locals. It is important therefore, to pave new avenues for bringing all this knowledge together in a multi-disciplinary way as it is the only way to approach these events and understand them in a holistic way.

Acknowledgements. The authors are grateful to Jacobs for providing a Flood Modeller licence for educational purposes and allowing us to undertake this research. Additionally, we would like to show our gratitude to Antoni Quetglas, Sóller Municipal Archivist, for his help in accessing the newspaper's data and bridge blueprints.

REFERENCES

Alcoverro, J., Corominas, J., Gomez, M., 1999. The Barranco de Arás flood at 7 august 1996 (Biescas, Central Pyrenees, Spain). Engineering Geology, 51, 10, 237–255.

AMS, 2021. Projectes de construcció i reparació de ponts. Folder 4387. Arxiu Municipal de Sóller (AMS).

Barriendos, M., Llasat, M.C., 2003. The case of the Maldà anomaly in the Western Mediterranean basin (AD 1760-1800): an example of strong climatic variability. Climatic Change, 61, 191–216.

BMS, 2021a. Collecció Setmanari Sóller, nº 4542, April 4th 1974. Biblioteca Municipal de Sóller (BMS). Consulted on: 25 September 2021.

BMS, 2021b. Collecció Setmanari Sóller, nº 4544, April 20th 1974. Biblioteca Municipal de Sóller (BMS). Consulted on: 25 September 2021.

Clark, D., 2011. How will climate change affect rainfall? Available at: https://www.theguardian.com/environment/2011/dec/15/climate-change-rainfall. [Accessed on 18 April 2021]

Cos, J., Doblas-Reyes, F., Jury, M., Marcos, R., Bretonnière, P-A, Samsó, M., 2022. The Mediterranean climate change hotspot in the CMIP5 and CMIP6 projections. Earth System Dynamics, 13, 321–340.

Costa, J.E., 1987. Comparison of the largest rainfall-runoff floods in the United States with those of the People's Republic of China and the world. Journal of Hydrology, 96, 1–4, 101–115.

Creutin, J.D., Borga, M., 2003. Radar hydrology modifies the monitoring of flash floods. Hydrological Processes, 17, 1453–1456.

Elleder, L., 2010. Reconstruction of the 1784 flood hydrograph for the Vltava River in Prague, Czech Republic. Global and Planetary Change, 70, 117–124.

Elleder, L., Herget, J., Roggenkamp, T., Niessen, A., 2013. Historic floods in the city of Prague—A reconstruction of peak discharges for 1481-1825 based on documentary sources. Hydrology Research, 44, 202–214.

Gaume, E., Borga, M., 2008. Post-flood field investigations in upland catchments after major flash floods: proposal of a methodology and illustrations. J. Flood Risk Management, 1, 175–189.

Gaume, E. et al., 2009. A collation of data on European flash floods. Journal of Hydrology, 367, 70–78.

Gaume, E. et al. Sub-chapter 1.3.4. Mediterranean extreme floods and flash floods. In: The Mediterranean region under climate change: A scientific update [online]. Marseille: IRD Éditions, 2016 (generated 30 mars 2022). Available on the Internet: <http://books.openedition.org/irdeditions/23181>. ISBN: 9782709922203. DOI: https://doi.org/10.4000/books.irdeditions.23181

Google Earth., 2021. Plan view of Soller and model river cross sections. Google Earth[online]. Available at: https://earth.google.com/web/. [Accessed on: 18 November 2021].

Herget, J., Meurs, H., 2010. Reconstructing peak discharges for historic flood levels in the city of Cologne, Germany. Global and Planetary Change, 70, 108–116.

Herget, J., Roggenkamp, T., Krell, M., 2014. Estimation of peak discharges of historical floods. Hydrology and Earth System Sciences, 18, 4029–4037. DOI: 10.5194/hess-18-4029-2014

IDEIB, 2021. Digital Elevation Model of the Balearic Islands. Available from: http://ideib.caib.es/cataleg/srv/cat/catalog.search;jsessionid=18BCF32A72E2E70D3D78E0177870BC3A#/metadata/16A574B8-7099-4E04-8757-71BF0BEB1786 [Accessed 18 November 2021]

Jacobs., 2020. Flood Modeller (v4.6.7) [computer programme]. Available from: Flood Modeller | Industry leading flood modelling software [Accessed 16 February 2022].

Llasat, M.C. et al., 2016. Flash floods trends versus convective precipitation in a Mediterranean region. Journal of Hydrology. DOI: 10.1016/j.jhydrol.2016.05.040

Mahmood, S., Khan, A., Ullah, S., 2016. Assessment of 2010 flash flood causes and associated damages in Dir Valley, Khyber Pakhtunkhwa Pakistan. International Journal of Disaster Risk Reduction [Online], 16, 215–223. doi.org/10.1016/j.ijdrr.2016.02.009

Moel, H., van Alphen, J., Aerts, J.C.J.H., 2009. Flood maps in Europe - Methods, availability, and use. Natural Hazards and Earth System Science, 9, 2, 289–301. doi.org/10.5194/nhess-9-289-2009. [Accessed 08 March 2022]

Nunez, C., 2019. Floods Explained [online]. National Geographic. Available at: www.nationalgeographic.com/environment/natural-disasters/floods [Accessed 20 January 2021].

Pabon, C., 2019. How much force is needed to break a cubic metre of stone? Quora. Unpublished.

Romero-Díaz, M.A., López-Bermudez, F., 1987. Morfometría de redes fluviales: revisión crítica de los parámetros más utilizados y aplicación al Alto Guadalquivir. Papeles de Geografía (Física), 12, 47–62.

Rosselló-Geli, J., 2000. Cabals a la vall de Sóller: episodis d'escorrentia intensa. Master's Thesis. Universitat de les Illes Balears. Palma de Mallorca. 156 p.

Rosselló-Geli, J., 2021. Discussion of progress and summary of hydraulic model. Unpublished.

Rosselló-Geli, J., Cortés, M., 2021. La prensa local, fuente para el estudio de inundaciones: el semanario Sóller (Mallorca) de 1900 a 200. Ería, 2, 2, 207–222.

Rullan, J., 1885. Inundación de Sóller y Fornalutx. Imprenta Felipe Guasp, Palma de Mallorca.

Sene, K., 2013. Flash Floods Forecasting and Warning. 1st ed. Springer, New York.

Stamataki, I., Kjeldsen, T.R., 2021. Reconstructing the peak flow of historical flood events using a hydraulic model: The city of Bath, United Kingdom. Journal of Flood Risk Management, 14, 3, Article Number: e12719. DOI: doi.org/10.1111/jfr3.12719

Stamataki, I., Kjeldsen, T., 2020. Hydraulic modelling of Bath's historical floods pre-Bath Flood Defence Scheme: Part 1 [Online]. Hydric-Bath. Available from: Hydraulic modelling of Bath's historical floods pre-Bath Flood Defence Scheme: Part I - HYDRIC-BATH (weebly.com) [Accessed 30 March 2021]

Tuel, A., Eltahir, E.A.B., 2020. Why is the Mediterranean a climate change hotspot? Journal of Climate, 33, 14, 5829–5843. DOI: https://doi.org/10.1175/JCLI-D-19-0910.1

Werner, M., Cranston, M., 2009. Understanding the value of radar rainfall nowcasts in flood forecasting and warning in flashy catchments. Meteorological Applications, 16, 1, 41–55.

Wetterzentrale. Atmospheric situation March 29th 1974. Available at: http://wetterzentrale.de. [Accessed on: 15 November 2021]

Wheater, H.S., 2002. Progress in and prospects for fluvial flood modelling. Philosophical Transactions of the Royal Society of London Series A 360, 1409–1431.

Received 27 April 2022
Accepted 13 September 2022